Supplementary Information (SI)

Dependence of particle nucleation and growth on high molecular weight gas phase products during ozonolysis of α-pinene

J. Zhao[1,2], J. Ortega[2], M. Chen[1], P. H. McMurry[1], and J. N. Smith[2,3]

[1]Department of Mechanical Engineering, University of Minnesota, Minneapolis, Minnesota, 55455, USA

[2]Atmospheric Chemistry Division, National Center for Atmospheric Research, Boulder, Colorado, 80307, USA

[3]Department of Applied Physics, University of Eastern Finland, Kuopio 70211, Finland

The supplementary material contains four sections.

Section I: contain**s** 3 tables and 6 figures.

Table S1. Summary of experimental conditions in this study.

Exp.	α-pinene	Ozone		Cluster CIMS reagent ions
	(ppb)	first 3 hours (ppb min^{-1})	steady state (ppb)	
E1	20	0.2	75	Nitrate dimer
E2	5	0.1	50	Nitrate dimer
E3	20	N/A	75	Acetate dimer

Table S2. Summary of all measured Category II products for *E1*: ion (m/z), peak concentration (in cm^{-3}), corresponding neutral identities, and correlation coefficients with > 20 nm particles.

Ion (m/z)	Peak conc.[a] (cm^{-3})	NO_3^- Clusters? [b]	Corresponding neutral[b]		Correlation coefficient[c]
			Mass (amu)	Formula	
142	2.5×10^5				0.63
158	2.1×10^5				0.67
228	3.0×10^5				0.66
240	4.2×10^6	Y	178	$C_5H_6O_7$	0.80
241	3.9×10^5				0.60
257	2.6×10^5				0.75
282	8.9×10^5	Y	220	$C_7H_8O_8$ or $C_8H_{12}O_7$	0.51
287	5.2×10^5				0.82
297	5.3×10^5				0.81
298	4.3×10^5	Y	236	$C_8H_{12}O_8$	0.69
308	2.6×10^6	Y	246	$C_{10}H_{14}O_7$	0.78
309	5.2×10^5				0.66
310	1.1×10^6	Y	248	$C_9H_{12}O_8$ or $C_{10}H_{16}O_7$	0.77
326	7.5×10^5			$C_9H_{12}O_9$ or $C_{10}H_{16}O_8$	0.61
327	5.5×10^5				0.80
329	2.5×10^5				0.82
339	8.0×10^5				0.72
341	4.6×10^5				0.61
343	3.0×10^5				0.50
355	5.5×10^5				0.74
356	4.3×10^5	Y	294	$C_{10}H_{14}O_{10}$	0.61
371	3.1×10^5				0.53
375	2.0×10^5				0.57

[a] Concentration: background subtracted peak concentration (in cm^{-3}) at time c in Fig. 1b;

[b] from Ehn et al. 2012;

[c] Correlation was performed with the concentration of >20 nm particles for time period t=0-10 hr in Fig. 1b (t=0 was defined as the time when ozone was added to the chamber).

Table S3. Summary of all measured m/z of category III products for *E1*.

Ion (m/z)
152, 154, 160, 164, 165, 166, 167, 168, 178, 179, 180, 182, 183, 192, 194, 196, 198, 206, 208, 209, 210, 212, 213, 214, 217, 218, 220, 222, 223, 224, 225, 226, 227, 234, 235, 236, 238, 239, 244, 246, 248, 249, 250, 251, 252, 253, 254, 262, 264, 265, 266, 267, 268, 270, 277, 278, 279, 280, 281, 285, 292, 293, 294, 295, 296, 307, 311, 313, 314, 324, 325 ,357

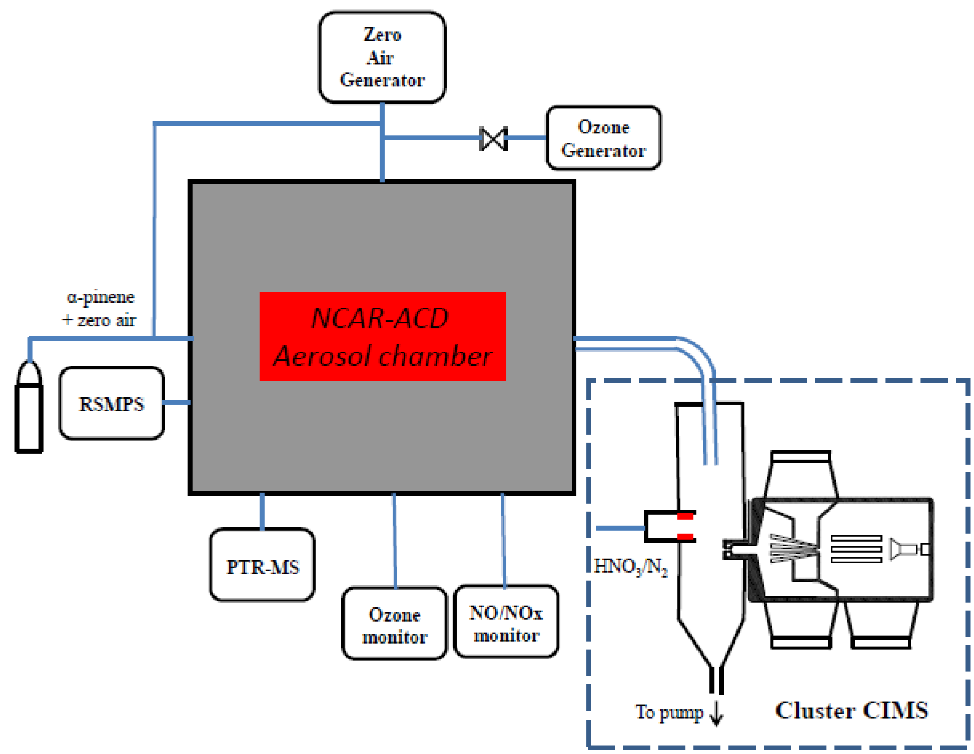

Fig. S1. Schematic diagram of the NCAR reaction chamber and the instruments used in this study.

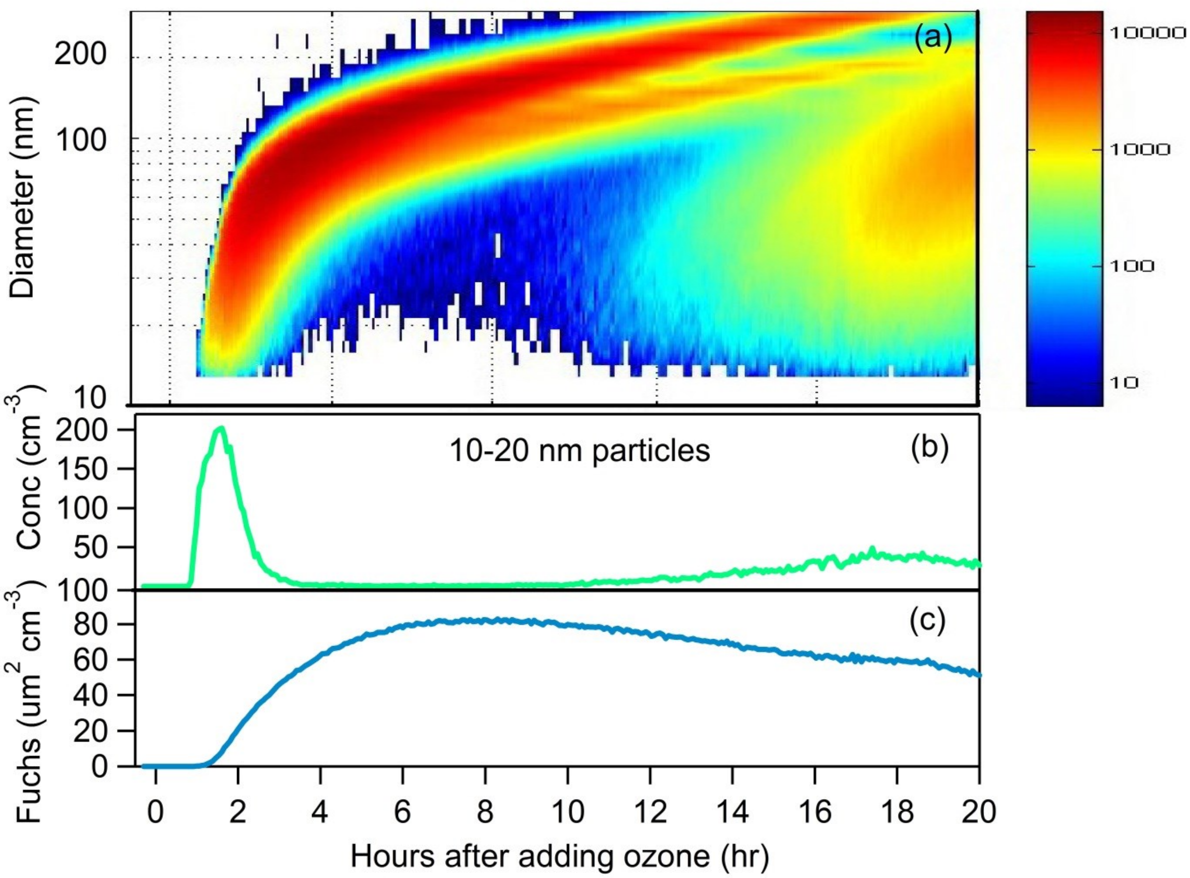

Fig. S2. Characteristics of particle formation from chamber α-pinene ozonolysis for *E2*: (a) Contour plot of the particle size distribution measured with the SMPS in the 10-350 nm diameter range; (b) Temporal total concentration of 10-20 nm particles; (c) Estimated time-dependent Fuchs surface area (in μm^2 cm^{-3}).

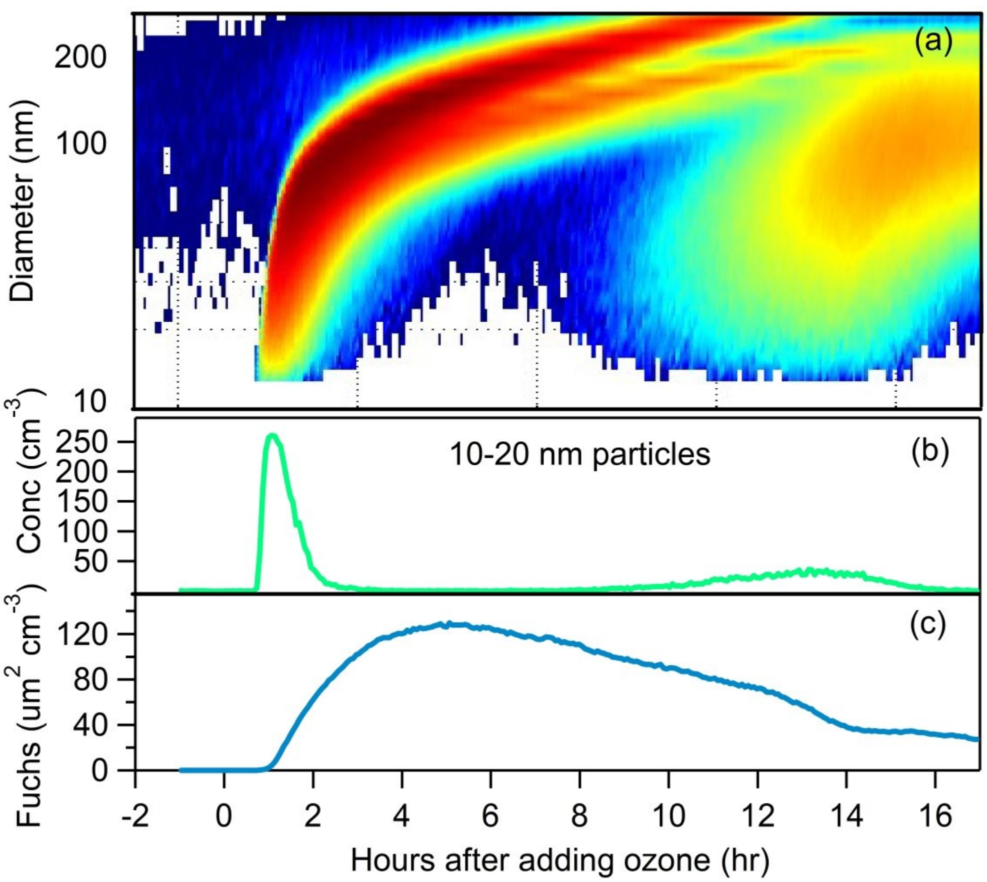

Fig. S3. Characteristics of particle formation from chamber α-pinene ozonolysis for *E3*: (a) Contour plot of the particle size distribution measured with the SMPS in the 10-350 nm diameter range; (b) Temporal total concentration of particles between 10 and 20 nm; (c) Estimated time-dependent Fuchs surface area (in μm^2 cm^{-3}).

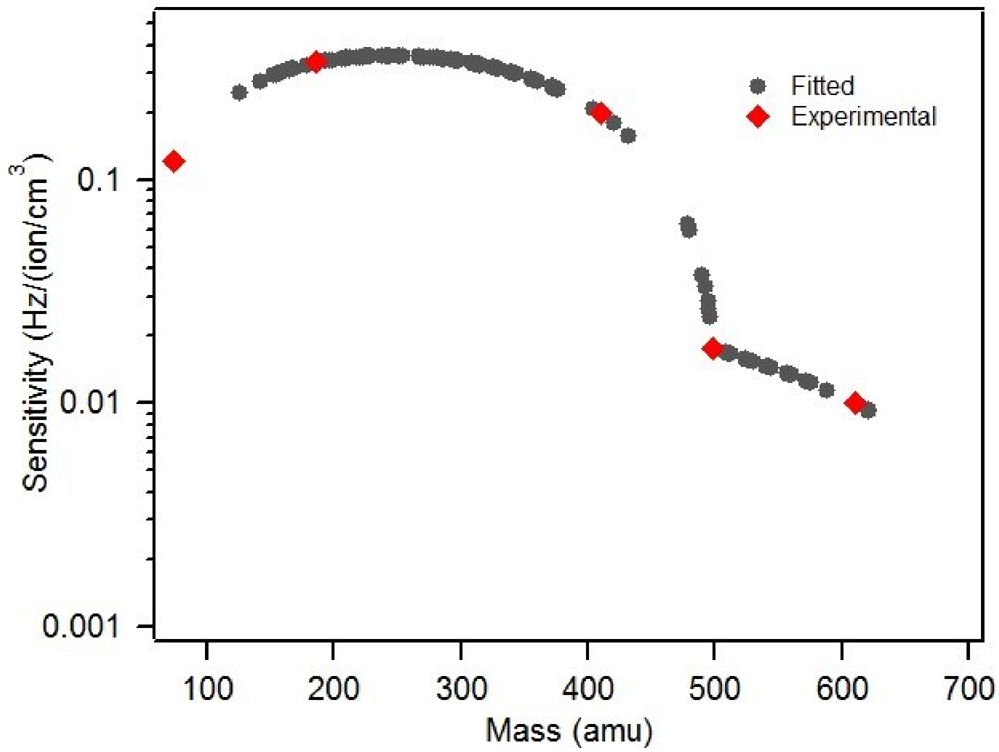

Fig. S4. Mass-dependent sensitivities used for estimating concentrations of oxidation products (Zhao et al., 2010).

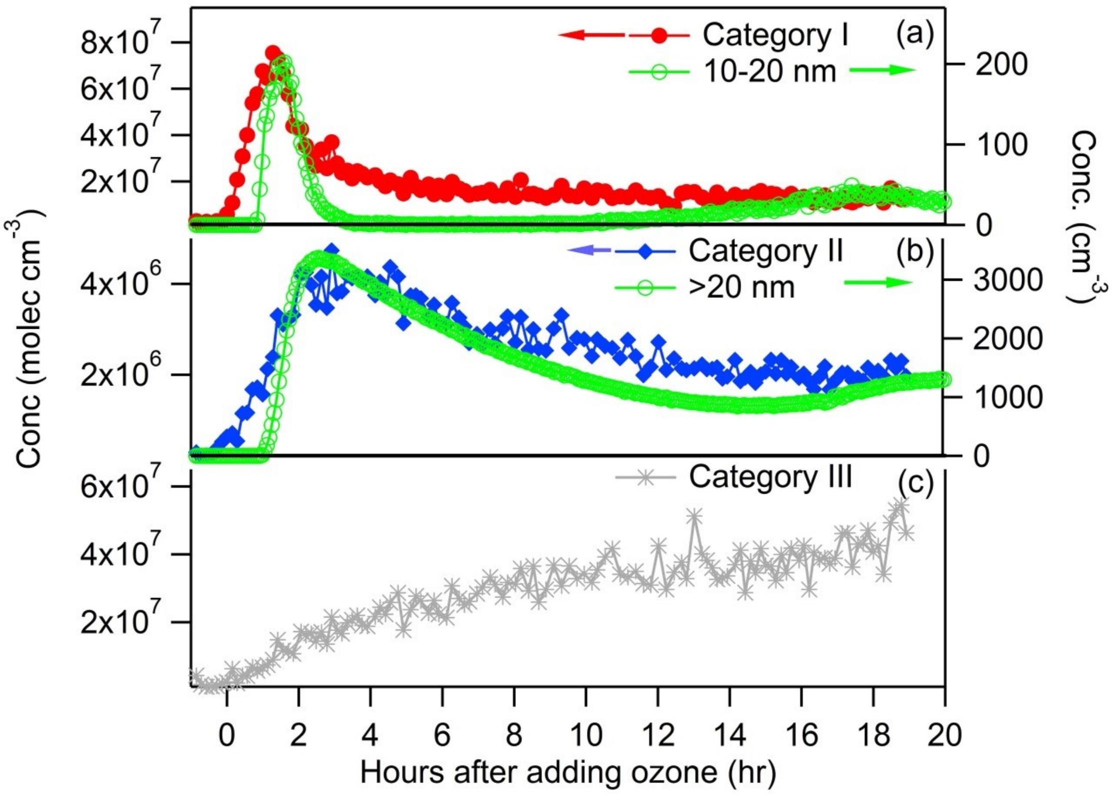

Fig. S5. Time-dependent total concentrations of the category I-III products measured with the Cluster CIMS, along with the total concentrations of 10-20 nm particles and particles larger than 20 nm measured with the SMPS for *E2*. (a) Category I products and 10-20 nm particles; (b) Category II products and particles larger than 20 nm; (c) Category III.

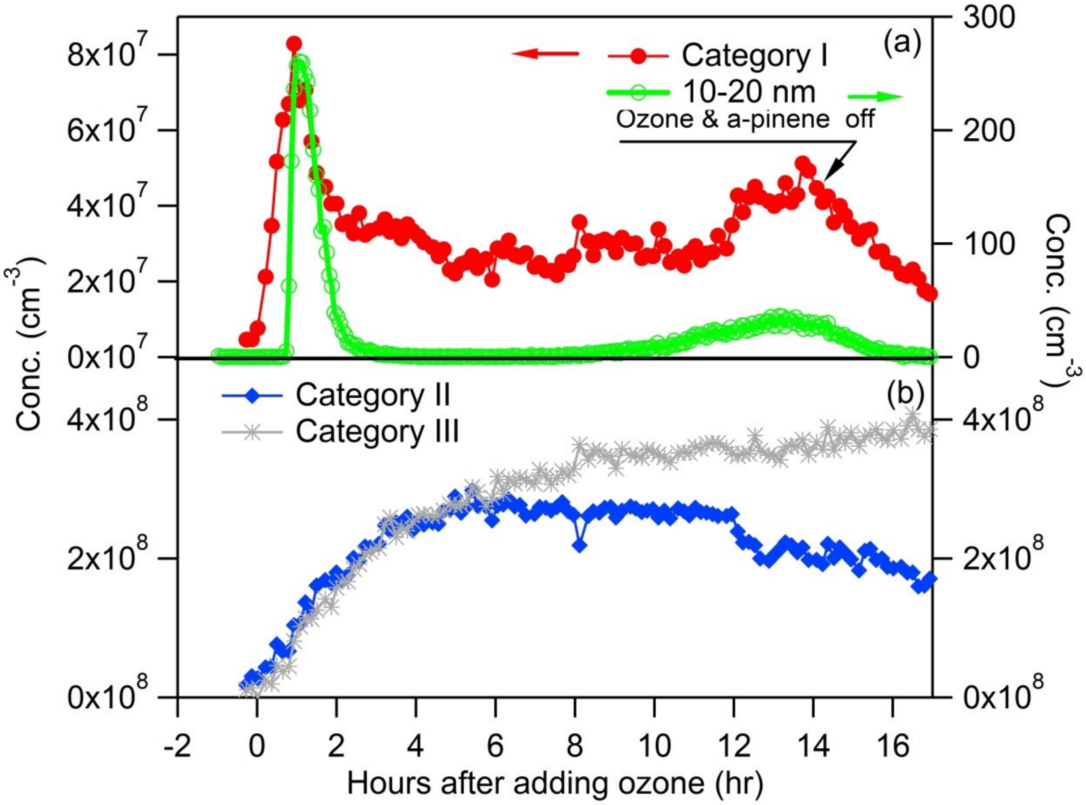

Fig. S6. Time-dependent total concentrations of the category I-III products measured with the Cluster CIMS, along with the total concentrations of 10-20 nm particles measured with the SMPS for *E3*. (a) Category I products and 10-20 nm particles; (b) Category II and III products.

Section II: This section describes the method used to estimate the formation and growth rates of the first and second events for *E1-E3*.

1. Method:

The evolution of particle concentrations between 10 nm and 20 nm can be estimated from the following general dynamic equation (eq. 1) (Gelbard and Seinfeld, 1974).

$$\frac{dN_{10-20}}{dt} = J_{10nm} - J_{20nm} + CoagSrc - CoagSnk \qquad (1)$$

$\frac{dN_{10-20}}{dt}$ is the rate of change of particle concentrations between 10 and 20 nm. For *E1-E3*, this rate was assumed to increase was linearly with time during the first half an hour when nucleation occurs. Thus it can be approximated as $\frac{\Delta N_{10-20}}{\Delta t}$, the concentration change divided by the time (half an hour). J_{20nm} is the formation rate of particles at 20 nm, which can be expressed as $\left.\frac{dN}{dDp}\right|_{20nm} \cdot GR$.

GR is the modal growth rate at 20 nm, and is estimated with the method described by Stolzenburg (2005). $CoagSrc$ and $CoagSnk$ are the coagulation source and coagulation sink terms respectively. These two terms are calculated according to Kuang et al. (2012).

Rearranging eq. 1, the particle formation rate at 10 nm ($J_{10\text{nm}}$) can then be calculated by eq. 2.

$$J_{10nm} \approx \frac{\Delta N_{10-20}}{\Delta t} + \left.\frac{dN}{dDp}\right|_{20nm} \cdot GR - CoagSrc + CoagSnk \qquad (2)$$

2. Summary of particle formation rates and growth rates for *E1-E3*.

Table S4. Summary of formation rates and growth rates for *E1-E3*

Exp.	1st event		2nd event	
	Form. Rate (cm^{-3} sec^{-1})	Growth Rate ($nm\ hr^{-1}$)	Form. Rate (cm^{-3} sec^{-1})	Growth Rate ($nm\ hr^{-1}$)
E1	0.42	36	0.038	28
E2	0.28	16	0.026	12
E3	0.53	23	0.022	13

Section III: This section describes how to estimate the minimum concentrations for growth of particles at the measured growth rates for *E1-E3*.

The minimum concentration of a monomer N1 required to grow particles at a certain rate can be estimated by eq. 3. (Kuang et al., 2010).

$$GR = \frac{1}{2} v_1 N_1 \bar{c} \qquad (3)$$

Where GR is the diameter growth rate, ν_l is the molecular volume for monomer and $\bar{c}$ is the thermal velocity of the monomer. A molecular weight of 500 amu is assumed for Category I products.

Table S5. Summary of minimum concentrations of a low molecular weight vapor (i.e. $N1=N_{98amu}$) or a high molecular weight vapor (i.e. $N1=N_{500amu}$) required to grow particle at the observed growth rates for *E1-E3*

Exp.	1st event		2nd event	
	N_{98amu} (cm^{-3})	N_{500amu} (cm^{-3})	N_{98amu} (cm^{-3})	N_{500amu} (cm^{-3})
E1	$8.3x10^8$	$3.3 x10^8$	$6.5 x10^8$	$2.5x10^8$
E2	$3.7 x10^8$	$1.4 x10^8$	$2.8 x10^8$	$1.1x10^8$
E3	$5.3 x10^8$	$2.1 x10^8$	$3.0 x10^8$	$1.2x10^8$

Section IV: This section describes the possible monomers for Category I products.

We assume that the dimers are formed either by hydrogen bonding or by covalent bonding that loses one water molecule. We can find the corresponding possible monomer for most of the high m/z peaks. There are also other pathways for the dimer formation that are not included in the table. It is also possible that some of the high m/z peaks are high molecular weight species rather than dimers of lower molecular weight compounds. The results are shown in Table S6.

Table S6. Possible monomers for Category I products.

Ion (m/z)	Neutral (amu)	Possible monomer I					Possible monomer II				
		Neutral (amu)	W/ NO_3^-	Cat.	W/ NO_3^- HNO_3	Cat.	Neutral (amu)	W/ NO_3^-	Cat.	W/ NO_3^- HNO_3	Cat.
328	266	133	195		258		142	204		267	III
330	268	134	196	III	259		143	205		268	III
340	278	139	201		264	III	148	210	III	273	
342	280	140	202		265	III	149	211		274	
358	296	148	210	III	273		157	219		282	II
359	234	117	179	III	242		126	188		251	III
372	310	155	217	III	280	III	164	226	III	289	
373	248	124	186		249	III	133	195		258	
374	312	156	218	III	281	III	165	227	III	290	
432	370	185	247		310	II	194	256		319	
460	398	199	261		324	III	208	270	III	333	
478	416	208	270	III	333		217	279	III	342	I
480	418	209	271		334		218	280	III	343	II
490	428	214	276		339	II	223	285	III	348	
492	430	215	277	III	340	I	224	286		349	
493	368	184	246	III	309	II	193	255		318	
494	432	216	278	III	341	II	225	287	II	350	
495	370	185	247		310	II	194	256		319	
496	434	217	279	III	342	I	226	288		351	
498	436	218	280	III	343	II	227	289		352	
510	448	224	286		349		233	295	III	358	I
511	386	193	255		318		202	264	III	327	II
512	450	225	287	II	350		234	296	III	359	I
523	398	199	261		324	III	208	270	III	333	
524	462	231	293	III	356	II	240	302		365	
525	400	200	262	III	325	III	209	271		334	
526	464	232	294	III	357	III	241	303		366	
530	468	234	296	III	359	I	243	305		368	
540	478	239	301		364		248	310	II	373	I
541	416	208	270	III	333		217	279	III	342	I
542	480	240	302		365		249	311	III	374	I
543	418	209	271		334		218	280	III	343	II
544	482	241	303		366		250	312		375	II
556	494	247	309	II	372	I	256	318		381	
557	432	216	278	III	341	II	225	287	II	350	
558	496	248	310	II	373	I	257	319		382	
559	434	217	279	III	342	I	226	288		351	
560	498	249	311	III	374	I	258	320		383	
574	512	256	318		381		265	327	II	390	
575	450	225	287	II	350		234	296	III	359	I
588	526	263	325	III	388		272	334		397	
590	528	264	326	II	389		273	335		398	
620	558	279	341	II	404		288	350		413	
621	496	248	310	II	373	I	257	319		382	

References:

Gelbard, F., Seinfeld J. H.: Numerical-Solution of Dynamic Equation for Particulate Systems, J. Comput. Phys., 28, 357-375, 1978.

Kuang, C., Riipinen, I., Sihto, S. L., Kulmala, M., McCormick, A. V., McMurry, P. H.: An improved criterion for new particle formation in diverse atmospheric environments, Atmos. Chem. Phys., 10, 8469-8480, 2010.

Kuang, C., Chen, M., Zhao, J., Smith, J., McMurry, P. H., and Wang J.: Size and time resolved growth rate measurements of 1 to 5 nm freshly formed atmospheric nuclei, Atmos. Chem. Phys., 12, 3573-3589,2012.

Stolzenburg, M. R., McMurry, P. H., Sakurai, H., Smith, J. N., Mauldin, R. L., Eisele, F. L., Clement, C. F.: Growth rates of freshly nucleated atmospheric particles in Atlanta, J. Geophys. Res., 110, D22S05, doi:10.1029/2005JD005935, 2005.

Zhao, J., Eisele, F. L., Titcombe, M., Kuang, C. G., and McMurry, P. H.: Chemical ionization mass spectrometric measurements of atmospheric neutral clusters using the cluster-CIMS, J. Geophys. Res., 115, D08205, doi:10.1029/2009JD012606, 2010.